American Mineralogist, Volume 88, pages 527–533, 2003

Stepwise dehydration of Sr-exchanged heulandite: A single-crystal X-ray study

NICOLA DÖBELIN* AND THOMAS ARMBRUSTER

Laboratorium für chemische und mineralogische Kristallographie, Universität Bern, Freiestrasse 3, CH-3012 Bern, Switzerland

ABSTRACT

A Sr-exchanged heulandite crystal of composition $Sr_{4.35}Ca_{0.13}(Al_{8.96}Si_{27.04}O_{72})\cdot 26H_2O$ was used for stepwise dehydration experiments. The crystal was heated for approximately 12 h from room temperature to 250 °C in steps of 50 °C using an airflow-heater device. For single-crystal X-ray data collection the crystal was quenched to –173 °C with liquid-N_2 on the diffractometer. Due to pronounced Sr order deviating from the topological symmetry *C*2/*m*, the structure was refined in space group *Cm* for each dehydration state. The initial H_2O content of 26 molecules per formula unit (pfu) at room temperature decreased to 17 molecules pfu after heating at 250 °C. Heating to 270 °C mechanically destroyed the crystal and a completely dehydrated state could not be studied. The loss of H_2O and accompanying migration of Sr caused a change of cell parameters: *a* and *c* slightly decreased, *b* decreased, and β remained invariant, leading to a reduction of the cell volume. As Sr loses H_2O upon dehydration, it moves toward the C rings and forms stronger bonds to the tetrahedral framework. With increasing dehydration the A and B ring become slightly compressed and elongated. Initially highly populated Sr sites split into less populated sites caused by the loss of surrounding H_2O molecules.

INTRODUCTION

Clinoptilolite and heulandite (structure code HEU) are zeolite minerals with cell parameters $a \approx 17.7$, $b \approx 17.9$, $c \approx 7.4$ Å, $\beta \approx 116°$. They are isostructural and possess topological monoclinic symmetry *C*2/*m*. The structure is characterized by a two-dimensional system of large channels composed of eight- and ten-membered tetrahedral rings, commonly named channel A (parallel to the **c** axis, ten-membered ring) and channel B (parallel to the **c** axis, eight-membered ring), respectively (Stolz et al. 2000). The A and B channels are crosslinked by eight-membered C channels running parallel to the **a** axis and [102]. The distinctive feature of clinoptilolite and heulandite is the Si/Al ratio in the tetrahedral framework (Bish and Boak 2001; Coombs et al. 1997). Silica-rich crystals with Si/Al ≥ 4.0 are called clinoptilolite, and more aluminous samples with Si/Al < 4.0 are called heulandite. The highest Si/Al ratio found in clinoptilolite is 5.7, and heulandite samples with the highest Al content found in nature have Si/Al ratios of 2.6 (Bish and Boak 2001).

Because of the low price and the availability of large quantities from sedimentary deposits (saline, alkaline lakes, deep-sea sediments, and low-temperature tephra systems: Hay and Sheppard 2001), clinoptilolite is mainly used for technological applications. However, due to the higher Al content in the tetrahedral framework heulandite samples show higher concentrations of extraframework cations and are usually of larger crystal size. Thus heulandite is more suitable for single-crystal X-ray diffraction experiments. Natural heulandite is mainly Ca-rich with approximate composition $(Na,K)Ca_4[Al_9Si_{27}O_{72}]\cdot 24H_2O$ (e.g., Armbruster and Gunter 2001).

Besides the four stable strontium isotopes ^{84}Sr, ^{86}Sr, ^{87}Sr, and ^{88}Sr, 22 radiogenic isotopes exist, of which ^{90}Sr has the longest half life (28.5 years). The stable isotopes are not harmful to the environment. However, the radioactive isotopes ^{89}Sr and ^{90}Sr are regarded as being among the most dangerous radioactive elements for organisms. In metabolic reactions Sr^{2+} behaves in a similar fashion to Ca^{2+}, which is an essential element in most organisms. Thus the radioactive element is incorporated in teeth and bone marrow of mammals where it emits 0.5 MeV β-radiation. Although the destructive effect of β-radiation is restricted to short ranges, ^{90}Sr forms a major hazard to the human body due to uptake by the organism and the short distance to the blood-forming marrow. The most frequent diseases caused by radioactive Sr contamination are bone cancer and leukemia (Ender et al. 1996).

Large quantities of radioactive Sr isotopes were released to the atmosphere and biosphere during tests of nuclear weapons and accidents in nuclear power plants (Kühn 1996; Monetti 1996), and 30–40 times the radioactivity of the atomic bombs dropped on Hiroshima and Nagasaki were released to the environment during the Chernobyl disaster (Armbruster 2001). A large area had to be decontaminated of the radioactive isotopes ^{137}Cs and ^{90}Sr. About 500 000 tons of zeolites (mainly clinoptilolite) were used for the construction of protective barriers and for agricultural applications in the contaminated areas (Chelishchev 1995). Clinoptilolite filtration of the drainage water of the encapsulated Chernobyl nuclear power plant reduced ^{137}Cs contents by 95% and ^{90}Sr concentrations by 50–60% (Tarasevich 1996).

Due to the low price and the high selectivity for the fission products ^{90}Sr and ^{137}Cs, zeolite minerals (mainly clinoptilolite

* E-mail: ndoebelin@gmx.ch

and chabazite) are used in large-scale applications for the treatment of contaminated wastewaters. Comparative studies of zeolite and Crystalline Silico-Titanate (CST), in its engineered form Ionsiv™IE-911, show a greater sorption capacity of CST for Sr. However, the material is more expensive than zeolite and thus is not economic at this stage of technological development (Bostick 1999; Bostick and DePaoli 1999).

The Sr concentration of natural heulandite is often high compared to other minerals—even zeolites—of the same mineral assemblage. Heulandites from Gibelsbach (Valais, Switzerland) contain 2.10 wt% SrO (0.55 Sr pfu), whereas chabasite, laumontite, stellerite, epistilbite, and scolecite in fissures of the same host rock contain at most 0.81 wt% SrO (Armbruster et al. 1996). Even higher Sr concentrations were found in amygdaloidal heulandite samples from Campegli, Italy (2.10 Sr pfu) (Lucchetti et al. 1982) and Kozakov Hill, Czechoslovakia (1.24 Sr pfu) (Cerny and Povondra 1969).

O'Day et al. (2000) used EXAFS analysis of natural heulandite with Sr concentrations of 2000–4500 ppm to determine Sr-O distances. The first-shell Sr-O distances for Sr atoms coordinated by five water molecules and three framework O atoms was 2.62 Å at –200 °C, and 2.59–2.60 Å at room temperature. Sr^{2+} is assumed to substitute for Ca^{2+} in the B channel (O'Day et al. 2000).

Studies have also been performed on Sr exchange in clinoptilolite/heulandite (Stolz et al. 2000; Orechovska et al. 1999), and the effect of time, temperature, and Sr concentration upon Sr exchange in clinoptilolite (Palmer and Gunter 2001).

Dehydration experiments using heulandite with unmodified cation composition (Alberti and Vezzalini 1983; Armbruster and Gunter 1991) and using fully Cd-exchanged heulandite (Döbelin and Armbruster 2003) showed a collapse of the HEU framework due to the loss of H_2O molecules and the induced movement and newly formed bonds of the extraframework cations. In addition, at higher temperatures (360 °C in Alberti and Vezzalini 1983; 250 °C in Döbelin and Armbruster 2003) T-O-T bonds break, leading to an altered framework topology also known as the B-phase. As discussed by Alberti and Vezzalini (1983) and Döbelin and Armbruster (2003) the occurrence and the topology of this B-phase seems to depend on the ionic potential (charge over radius) of the extraframework cations.

The aim of this study is: (1) to monitor the loss of H_2O and the movement of Sr cations within the channels with increasing temperature, (2) to describe the framework topology at all dehydration states and to find potential phase transitions, and (3) to discuss the results in comparison with the results from Alberti and Vezzalini (1983) and Döbelin and Armbruster (2003).

Experimental procedure

A Sr-exchanged heulandite crystal of 0.46 × 0.24 × 0.18 mm in diameter from Nasik, India was used for the structure analysis. The cation exchange was performed in 3M $SrCl_2 \cdot 6H_2O$ at 150 °C for 7 weeks, resulting in crystals with composition $Sr_{4.35}Ca_{0.13}[Al_{8.96}Si_{27.04}O_{72}] \cdot nH_2O$ (determined by electron microprobe analysis; Stolz and Armbruster 2000). Single-crystal X-ray data were obtained with a Siemens SMART CCD diffractometer operating at 50 kV and 40 mA with graphite-monochromated Mo$K\alpha$ X-radiation. For data acquisition the crystal was quenched to –173 °C using a conventional liquid-N_2 cooling device to minimize rehydration and thermal vibration. Different dehydration states were obtained by in situ heating the crystal on the goniometer head to 100, 150, 200, 250, and 270 °C for 12–18 hours with an airflow heater. The structure was refined for each dehydration state.

Data collection was performed with the standard hemisphere setup and a crystal-to-detector distance of 5.439 cm with corresponding resolution 0.78 Å (resolution = $\frac{\lambda}{2 \cdot \sin(\theta)}$). Orientation matrices and cell parameters were retrieved from 75 frames using the SMART software (Siemens 1995). The program SAINT (Siemens 1995), which corrects for Lorentz and polarization effects, was used to reduce the data. The structures were refined by a least-squares method on F^2 using SHELX-97 (Sheldrick 1997) and neutral atom scattering factors (Si for T sites).

Structure refinements were performed in space group $C2/m$ and the subgroups $C2$, Cm, and $C\bar{1}$, but only Cm yielded reasonable $R1$ values of 3.38–4.73% for dehydration states up to 200 °C. Refinements in space group $C2/m$ converged at $R1$ values of ca. 9–10%. In particular, low-intensity reflections could not be properly modeled in space group $C2/m$. Possible twinning by the inversion operation was considered in the Cm refinement and was determined to lie below 10%. The tetrahedral framework shows pseudo-$C2/m$ symmetry. Pairs of pseudosymmetrical equivalents are labeled with the same symbol (T for tetrahedral sites, O for tetrahedral O atom ligands) and the same number. One site, related to another site by a pseudotwofold axis, is marked with an additional single quote (e.g., T1-T1'). The channel occupants do not necessarily have pseudosymmetric equivalent sites and are therefore labeled with a symbol (Sr for strontium, W for H_2O molecules) and a continuous number (Fig. 1). Sr sites were identified on the basis of low atomic displacement parameters and appropriate bonding distances to framework O atom sites. Table 1 shows the nomenclature of the data sets of different dehydration states, as well as additional information for the data collection.

Results

Loss of H_2O caused a change of the cell parameters: a and c decreased slightly, b decreased strongly, and β remained more or less the same (Table 1). This is mostly in agreement with the results of Döbelin and Armbruster (2003), Alberti and Vezzalini (1983), and Armbruster and Gunter (1991). The H_2O content decreased from 26 molecules per formula unit (pfu) in srh3_rt and srh3_100, to 19 in srh3_150, 18 in srh3_200, and 17 in srh3_250. A fully dehydrated structure could not be achieved. Many reflections in structure srh3_250 were split into two subreflections. Heating to 250 °C split the crystal into several fragments that were visible with the adjustment scope. Heating to 270 °C mechanically destroyed the crystal. All data sets were refined in space group Cm leading to $R1$ values of 3.83–4.73% (srh3_rt-srh3_200), and 10.17% (srh3_250). At higher temperatures the A and B channels became slightly compressed and elongated (Table 2), but a heat-collapsed phase with an obvious rearrangement of T-O-T angles and channel dimensions at a well-defined temperature (as found by Döbelin and

TABLE 1. Data collection at –173 °C and refinement parameters for heulandite-Sr

Composition*	$Sr_{4.35}Ca_{0.13}[Al_{8.96}Si_{27.04}O_{72}]\cdot nH_2O$				
Crystal size (mm)	0.46 × 0.24 × 0.18				
Radiation	Mo*K*α				
Scan type	hemisphere				
Sample name	srh3_rt	srh3_100	srh3_150	srh3_200	srh3_250
Dehydration temp.	room temp.	100 °C	150 °C	200 °C	250 °C
a (Å)	17.714(2)	17.698(3)	17.643(3)	17.642(3)	17.60(1)
b (Å)	18.000(3)	17.970(3)	17.842(3)	17.775(3)	17.59(1)
c (Å)	7.430(1)	7.426(1)	7.418(1)	7.414(1)	7.408(5)
β (°)	116.627(3)	116.653(2)	116.851(2)	116.897(2)	116.76(1)
Space group	*Cm*	*Cm*	*Cm*	*Cm*	*Cm*
n(H_2O)	26	26	19	18	17
Measured reflections	5813	5792	5702	5644	3739
Unique reflections	3058	3043	3015	3008	2330
Observed refl. > 4σ	2763	2724	2541	2460	1629
No. of parameters	331	331	344	353	323
Rint (%)	3.54	3.58	3.62	3.59	4.99
R1 (%)	3.83	3.97	4.42	4.73	10.17
wR2 (%)	9.93	10.32	11.92	12.95	25.79
GooF	1.007	1.018	1.018	1.065	2.024

* Determined by electron-microprobe analysis.

$$R1 = \left(\sum \left||F_0| - |F_c|\right|\right) / \left(\sum |F_0|\right) \quad wR2 = \sqrt{\left(\sum w \cdot \left(F_0^2 - F_c^2\right)\right) / \left(\sum w \cdot \left(F_0^2\right)^2\right)} \quad \text{GooF} = \sqrt{\left(\sum w \cdot \left(F_0^2 - F_c^2\right)^2\right) / (n-p)}.$$

TABLE 2. Diameters of the A and B channels (a × b), in angstroms, measured from the centers of tetrahedra ligands at different dehydration states

	A channel	B channel
Room temperature	10.4 × 5.8	7.4 × 6.2
100 °C	10.4 × 5.8	7.3 × 6.3
150 °C	10.6 × 5.7	7.1 × 6.5
200 °C	10.7 × 5.6	7.1 × 6.6
250 °C	10.6 × 5.5	7.1 × 6.5

Armbruster 2003, Alberti and Vezzalini 1983, and Armbruster and Gunter 1991) was not seen. The presence of a relatively large amount of H_2O in sample srh3_250 (17 molecules pfu) indicates that the temperature was not high enough to cause complete dehydration. Atomic coordinates, interatomic bond distances, and anisotropic displacement parameters for all structures are listed in Tables 3–12[1].

DISCUSSION

Initial structure at room temperature

Structure refinements of HEU-topology structures are commonly performed in space group *C*2/*m*. Note that previous refinements of the Sr-exchanged heulandite sample (from the same batch as our material) were also refined in space group *C*2/*m* (Stolz and Armbruster 2000). However, the asymmetrical Si, Al preference of certain framework sites lowers the symmetry and also affects the distribution of extraframework cations within the channels, which bond preferentially to framework O atoms linked to an Al tetrahedron. The problem of symmetry lowering in heulandite has been addressed by Armbruster (2001). Tetrahedra with high Al content can be identified by analysis of T-O bond lengths. The Si-O distance in tetrahedral coordination amounts to 1.61 Å, and Al-O to 1.75 Å, as known from feldspar structure analysis (Kunz and Armbruster 1990). With a mean T-O distance of 1.673(4) Å, T2' shows the highest Al concentration in srh3_rt, followed by T1', T2, T3, and T4, with mean T-O distances in the range 1.636(5) to 1.654(4) Å. Thus Al is mainly accumulated in the areas around T2' and T2 (Fig. 2). The low-symmetry Si, Al distribution is also reflected in the arrangement of extraframework Sr cations.

Sr1 (population 76%) in the A ring has a less occupied pseudosymmetric counterpart Sr2 (population 46%). Sr1 has two bonds to the framework (2 × Sr1-O2': 2.71 Å). Notice that O2' forms a corner of T2' for which the highest Al content was derived. The pseudosymmetric equivalent Sr2 bonds to two O2 atoms forming corners of T2 tetrahedra, which are suggested to have a high Al content as well. However, the lower Al content of T2 compared to T2' causes weaker attractive forces and thus longer bonding distances between Sr2 and O2 (2.80 Å). Both Sr sites are additionally surrounded by five H_2O sites.

Sr3 (population 78%) in the B ring has no pseudosymmetric counterpart (Fig. 3). Sr4 is a satellite position of Sr3, only 0.57 Å away. The distance between Sr3 and the location of its potential pseudosymmetric equivalent is only 2.49 Å, and thus is too close for the simultaneous presence of Sr at both Sr3 and Sr4 and their counterpart. The sum of the occupancies of the Sr3 and Sr4 sites is 90%, therefore the potential symmetric-equivalent sites could have a maximum occupancy of 10%. In fact they are empty. The lack of pseudosymmetric counterparts to the highly populated Sr3 site is one important reason why structure refinements in space group *C*2/*m* were less successful than those in space group *Cm*. However, the major reason for space group *Cm* is partial Si, Al order, which has only slight bearing on the diffraction data, but directs the extraframework Sr arrangement. The atom at the Sr3 site bonds to framework

[1] For a copy of Tables 3–12, document item AM-03-028, contact the Business Office of the Mineralogical Society of America (see inside front cover of recent issue) for price information. Deposit items may also be available on the American Mineralogist web site at http://www.minsocam.org.

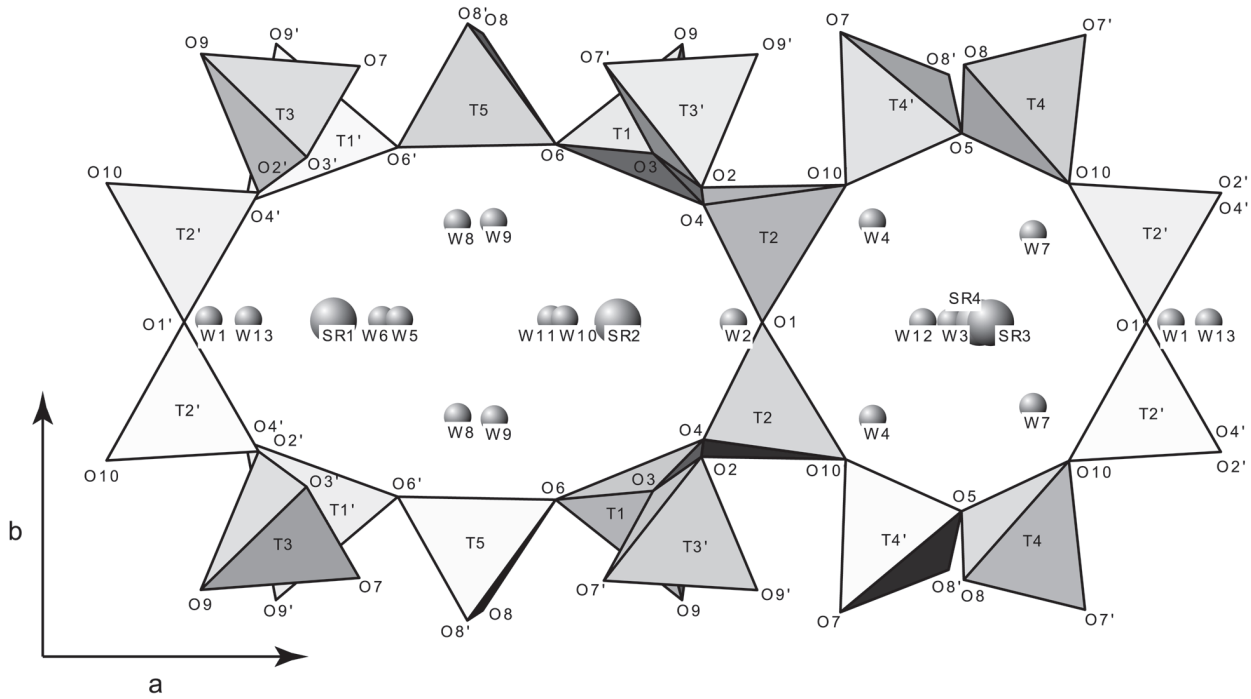

FIGURE 1. Polyhedral representation of the heulandite structure projected parallel to **c**. The ten-membered A channel (left) and the eight-membered B channel (right) of structure srh3_rt are displayed. All Sr sites are located on the mirror plane.

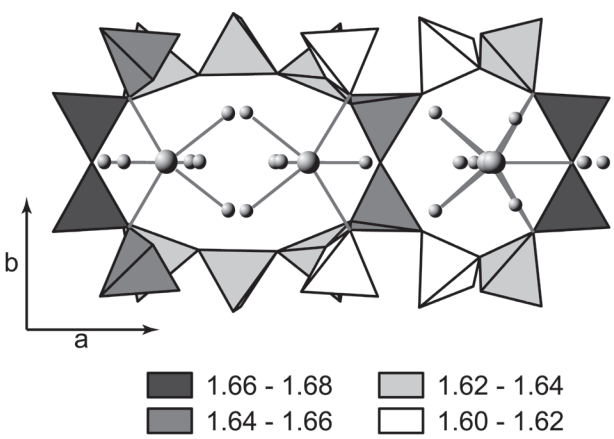

FIGURE 2. A and B ring of structure srh3_rt projected along [001], showing the mean T-O distance marked with shades of grey. The ideal Si-O distance in tetrahedral coordination is 1.61 Å; Al-O tetrahedra are noticeable larger and show bond lengths of 1.75 Å (Kunz and Armbruster 1990). A large mean T-O distance (dark gray) suggests a high Al content, whereas distances close to 1.61 Å suggest no Al substitution. Sr sites (large spheres) bond preferentially to O atoms linked to Al tetrahedra.

O atoms O1' (2.63 Å) and O10 (2×, 2.74 Å) of the Al-bearing tetrahedron T2', and to six H_2O molecules [Sr3-W3: 2.64 Å, Sr3-W4: 2.54 Å (2×), Sr3-W7: 2.57 Å (2×), and Sr3-W12: 2.57 Å] on the opposite side. Sr bond lengths to framework O atoms are slightly larger and those to H_2O oxygen atoms are smaller than the distances derived from EXAFS analysis (O'Day 2000). Sr4 shows the same bond configuration (Sr4-O1': 2.72 Å, Sr4-O10: 2.72 Å), but has a population of only 12%.

Dehydrated phases

Heating at 100 °C reduced H_2O populations slightly. Most affected were W8 and W10, each losing 9% occupancy at the H_2O sites. At 150 °C the occupancies of the H_2O sites decreased dramatically. Sites in the A channel (W6, W8, W11) lost more than 30% H_2O site occupancy. The lack of compensating bonds led to a partial migration of Sr toward the channel wall. Thus Sr1 split into Sr1 and Sr5, and Sr2 split into Sr2, Sr6, and Sr7. This migration toward the channel wall reduced the bonding distance from 2.83 Å (Sr2-O2) to 2.63 Å (Sr6-O2), and from 2.75 Å (Sr1-O2') to 2.56 Å (Sr5-O2'), respectively (Fig. 4). The sum of populations of these clusters remained equal to the initial populations. The W4 site in the B ring split into W4 and W4' sites, whereas the total population, as well as the population of W7, decreased by approximately 20%. W10 completely migrated to a new site labeled W11', and W13 disappeared. W2 was no longer detected, probably due to an overlap with the new Sr7 site (Figs. 4 and 5 show a comparison between the

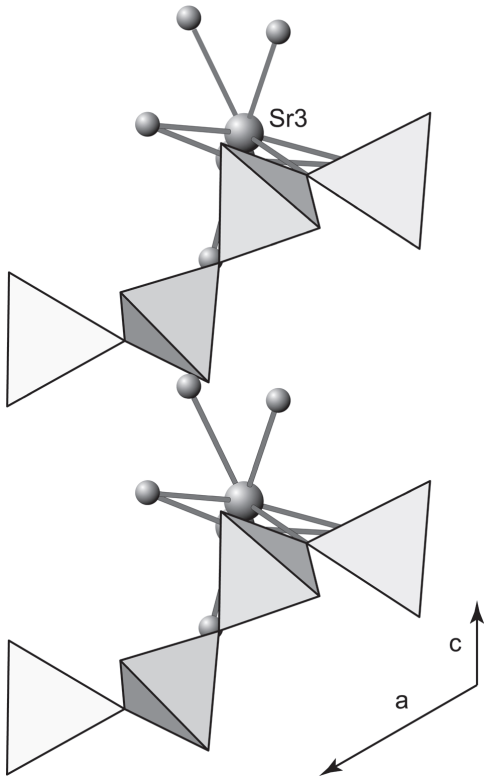

FIGURE 3. A projection along [010] of Sr3 in the B channel showing the void location of the pseudosymmetrical counterpart in srh3_rt. This is the main reason for the *Cm* symmetry of this structure.

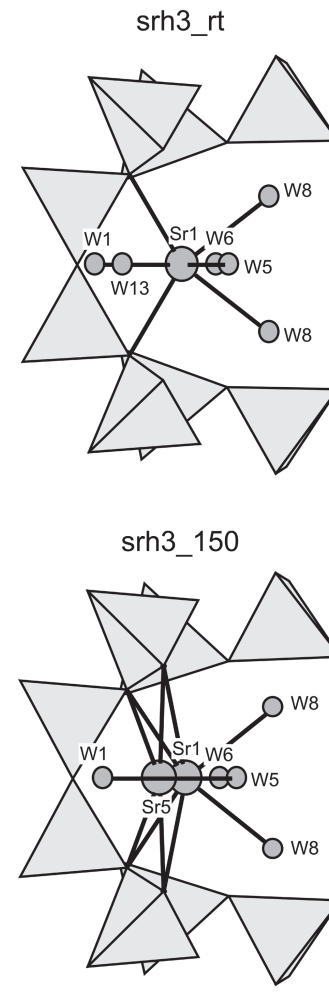

FIGURE 4. The splitting of the Sr1 site upon dehydration is shown in a projection parallel to [001]. At room temperature, this highly populated site bonds twice to the tetrahedral framework, and is coordinated by H_2O molecules on the opposite side. The loss of surrounding H_2O at 150 °C provokes splitting of the Sr1 site into the Sr1 and Sr5 sites, which both move slightly toward the center of the C ring. This allows atoms at both sites to bond to four tetrahedral framework O atoms.

structures at room temperature and at 150 °C).

The decrease of H_2O populations in the A ring continued in experiment srh3_200. The occupancies of W5, W8, and W9 decreased significantly leading to further splitting of Sr sites. W6 in the A channel and W12 in the B channel disappeared. All Sr sites in the A channel moved toward the center of the C channel. The pseudosymmetric equivalent Sr3' of Sr3 appeared with a low occupancy of 11%. The overall Sr content of the B channel decreased by 13%, which was balanced by an increase in the A channel. The highly disordered H_2O site W13 appeared in the B ring which bonds to the atom at the new Sr3' site and to Sr2 in the A channel. W7 split into W7 and W7', however, W7 became strongly disordered (high B_{eq} value). A new highly disordered site Sr8 in the A channel probably overlaps with W11' and W12'.

Three trends of Sr migration are seen after dehydration at 250 °C: (1) The population of Sr1 and Sr6 decreased to approximately 9% and 11%, respectively, while Sr1' moved toward the center of the A channel, forming a highly disordered site (probably overlapping W11' and W12') and bonding to W5 and W8; (2) Sr1 almost disappeared and the populations of Sr2' and Sr6' increased strongly; (3) rearrangement of populations in the B channel. Sr4 became the most populated site (29%), and Sr3 and Sr3' were more or less balanced with occupancies of 19% and 16%, respectively. The H_2O content decreased from 18 to 17 molecules pfu. W9 was no longer detected and W4 and W4' were combined in the disordered site W4'. W5 and W7' decreased strongly, while the population of W4', W7', and W13 increased, and a new site W14 appeared. The dehydration process up to 250 °C causes a slight distortion of the framework topology (see Table 2) leading to a decrease of the unit-cell volume from 2117.26 Å^3 in srh3_rt to 2047.64 Å^3 in srh3_250.

DISCUSSION

In contrast to the Cd-exchanged heulandite discussed by Döbelin and Armbruster (2003), Sr-exchanged heulandite showed no dramatic changes in both channel occupants and

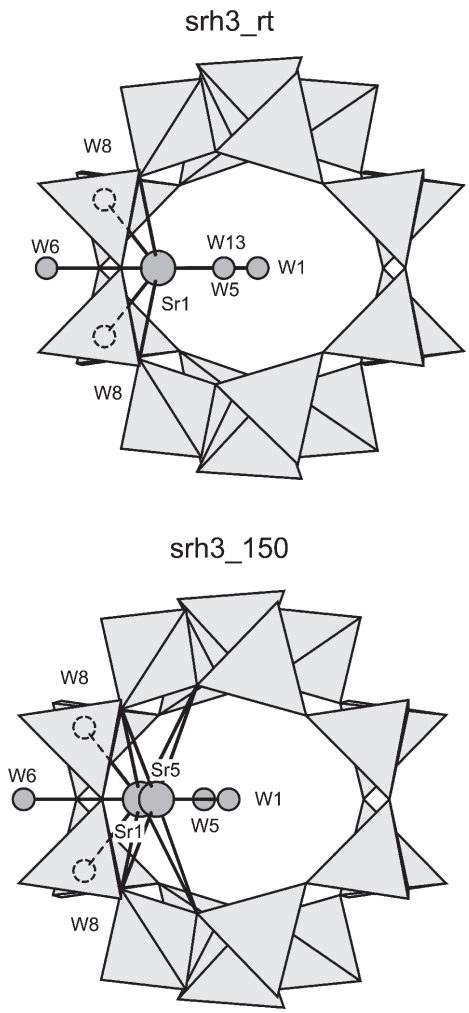

FIGURE 5. Splitting of the Sr1 site with advanced dehydration is also visible in a projection parallel to [100] (one of the eight-membered C channels). For the sake of clarity all Sr and H_2O sites except Sr1 and the surrounding areas are omitted.

framework topology. One possible explanation for this differing reaction upon dehydration is the lower ionic potential (charge / radius) of Sr^{2+} (1.52) compared to Ca^{2+} (1.75) and Cd^{2+} (1.83, based on radii in octahedral coordination taken from Shannon 1976). According to dehydration experiments on heulandites of natural cation composition (Alberti and Vezzalini 1983; Armbruster and Gunter 1991), and the results on heulandite-Cd by Döbelin and Armbruster (2003), this study confirms the supposition of a close relation between the ionic potential of extraframework cations and the occurrence of a collapse or a phase transition of the HEU framework. However, two points indicate that the temperature was too low for a complete dehydration, which is a precondition for a structural collapse: (1) The structure dehydrated at 250 °C still contained about 65% of the initial H_2O. At this hydration stage neither the unmodified samples (Alberti and Vezzalini 1983; Armbruster and Gunter 1991), nor the Cd-exchanged heulandite (Döbelin and Armbruster 2003) showed any dramatic changes of the structural topology. (2) The observation of the phase transition in heulandite-Cd (Döbelin and Armbruster 2003) showed that the main release of H_2O takes place in a relatively narrow temperature range, preceded by a constant but slow decrease of H_2O amount. This first stage of slow dehydration was also found in srh3. However, the expected sudden release of almost all H_2O was not seen, instead, the crystal lost its structural integrity and became unsuitable for X-ray diffraction analysis. We assume that this is caused by the expected strong dehydration starting at 250 °C, which causes strain in the framework that cannot be easily compensated by distortions of T-O-T angles and flipping of tetrahedra. It has also to be considered that the crystal is exposed to very high variations in temperature in a short period during the experiment (difference between dehydration and data collection in srh3_270: 443 °C), and that the thermal expansion and contraction contributes to the stress in the tetrahedral framework. This assumption will have to be proofed in subsequent studies.

Removal of radioactive elements (mainly Sr and Cs) from waste- and groundwater is an important application of natural zeolites. A review of common techniques and practical applications was published by Kalló (2001). Large amounts of contaminated material have to be deposited, still producing heat by fission of radioactive nuclei. Extensive knowledge about processes at raised temperatures, the rigidity of the crystal framework, and the stability of the extraframework cations and water molecules is essential in order to prevent a release of radioactivity to the environment.

ACKNOWLEDGMENTS

This study was supported by the Swiss 'Nationalfonds', credit 20-65084.01 to T. Armbruster. We acknowledge the constructive reviews by two anonymous referees.

REFFERENCES CITED

Alberti, A. and Vezzalini, G. (1983) The thermal behaviour of heulandites: a structural study of the dehydration of Nadap heulandite. Tschermaks Mineralogische und Petrographische Mitteilungen, 31, 259–270.

Armbruster, T. (2001) Clinoptilolite-heulandite: applications and basic research. In A. Galarnau, F. Di Renzo, F. Faujula, and J. Vedrine, Eds., Studies in Surface Science and Catalysis 135. Zeolites and Mesoporous Materials at the Dawn of the 21th Century, 13–27. Elsevier, New York.

Armbruster, T. and Gunter, M.E. (1991) Stepwise dehydration of heulandite-clinoptilolite from Succor Creek, Oregon, U.S.A.: A single-crystal X-ray study at 100 K. American Mineralogist, 76, 1872–1883.

——— (2001) Crystal structures of natural zeolites. In D.L. Bish and D.W. Ming, Eds., Natural Zeolites: Occurrence, Properties, Applications, vol. 45. p. 1–67. Reviews in Mineralogy and Geochemistry, Mineralogical Society of America, Washington, D.C.

Armbruster, T., Kohler, T., Meisel, T., Nägler, T., Götzinger, M.A., and Stalder, H.A. (1996) The zeolite, fluorite, quartz assemblage of the fissures at Gibelsbach, Fiesch (Valais, Switzerland): crystal chemistry, REE patterns, and genetic speculations. Schweizerische Mineralogische und Petrographische Mitteilungen, 76, 131–146.

Bish, D.L. and Boak, J.M. (2001) Clinoptilolite-heulandite nomenclature. In D.L. Bish and D.W. Ming, Eds., Natural Zeolites: Occurrence, Properties, Applications, vol. 45, 207–216. Reviews in Mineralogy and Geochemistry, Mineralogical Society of America, Washington, D.C.

Bostick, D.T. (1999) Fission product separations testing. Oak Ridge National Laboratory, Tennessee, TTP Number OR16C312.

Bostick, D.T. and DePaoli, S.M. (1999) Evaluation of improved techniques for the removal of fission products from process wastewater and groundwater: FY 1998 and 1999 status. Oak Ridge National Laboratory, Lockheed Martin, Tennessee, ORNL/TM-13689.

Černý, P. and Povondra, P. (1969) A polycationic strontian heulandite: comments on crystal chemistry and classification of heulandite and clinoptilolite. Neues Jahrbuch für Mineralogie Monatshefte, 349–361.

Chelishchev, N.F. (1995) Use of natural zeolites at Chernobyl. In D.W. Ming and F.A. Mumpton, Eds., Natural Zeolites '93, 525–532, International Committee on Natural Zeolites, Brockport, New York 14420.

Coombs, D.S., Alberti, A., Armbruster, T., Artioli, G., Colella, C., Galli, E., Grice, J.D., Liebau, F., Mandarino, J.A., Minato, H., Nickel, E.H., Passaglia, E., Peacor, D.R., Quartieri, S., Rinaldi, R., Ross, M., Sheppard, R.A., Tillmanns, E., and Vezzalini, G. (1997) Recommended nomenclature for zeolite minerals: Report of the Subcommittee on Zeolites of the International Mineralogical Association. Commission on New Minerals and Mineral Names, Canadian Mineralogist, 35, 1571–1606.

Döbelin, N. and Armbruster, T. (2003) Stepwise dehydration and change of framework topology in Cd-exchanged heulandite. Microporous and Mesoporous Materials, in press.

Ender, R., Fix, M., Iten, R., Pilloud, M., Rusch, C., Stampanoni-Panariello, A., and Zurmühle, D. (1996) Radioaktivität (Ionisierende Strahlung), Ein Leitprogramm. Institut für Verhaltenswissenschaften und Departement Physik, Eidgenössische Technische Hochschule Zürich.

Hay, R.L. and Sheppard, R.A. (2001) Occurrence of zeolites in sedimentary rocks: An overview. In D.L. Bish and D.W. Ming, Eds., Natural Zeolites: Occurrence, Properties, Applications, vol. 45, p. 217–234. Reviews in Mineralogy and Geochemistry, Mineralogical Society of America, Washington, D.C.

Kalló, D. (2001) Natural zeolites in water and wastewater treatment. In D.L. Bish and D.W. Ming, Eds., Natural Zeolites: Occurrence, Properties, Applications, vol. 45 of Reviews in Mineralogy and Geochemistry, 519–550, Mineralogical Society of America.

Kühn, M. (1996) Das Atomwaffenzeitalter beginnt. Greenpeace e. V., http://www.greenpeace.de/GP_DOK_3P/HINTERGR/C02HI04.HTM.

Kunz, M. and Armbruster, T. (1990) Difference displacement parameters in alkali feldspars: Effects of (Si,Al) order-disorder. American Mineralogist, 75, 141–149.

Lucchetti, G., Massa, B., and Penco, A.M. (1982) Strontian heulandite from Campegli (Eastern Ligurian ophiolites, Italy). Neues Jahrbuch für Mineralogie Monatshefte, 541–550.

Monetti, M.A. (1996) Worldwide deposition of strontium-90 through 1990. Vol. EML-579, Environmental Measurements Laboratory, U.S. Department of Energy, New York, http://www.eml.doe.gov/publications/reports/eml579.pdf.

O'Day, P.A., Newville, M., Neuhoff, P.S., Sahai, N., and Carroll, S.A. (2000) X-Ray absorption spectroscopy of strontium(II) coordination, I. Static and thermal disorder in crystalline, hydrated, and precipitated solids and in aqueous solution. Journal of Colloid and Interface Science, 222, 184–197.

Orechovska, J., Misaelides, P., Godelitsas, A., Rajec, P., Kleve-Nebenius, H., Noli, F., and Pavlidou, E. (1999) Investigation of HEU-type zeolite crystals after interaction with Sr^{2+} cations in aqueous solution using nuclear and surface analytical techniques. Journal of Radioanalytical and Nuclear Chemistry, 241, 519–527.

Palmer, J.L. and Gunter, M.E. (2001) The effects of time, temperature, and concentration on Sr^{2+} exchange in clinoptilolite in aqueous solutions. American Mineralogist, 86, 431–437.

Shannon, R.D. (1976) Revised effective ionic radii and systematic studies of interatomic distances in halides and chalcogenides. Acta Crystallographica, A 32, 751–767.

Sheldrick, G.M. (1997) SHELX-97, University of Göttingen, Germany.

Siemens (1995) ASTRO and SAINT. Data Collection and Processing Software for the SMART System.

Stolz, J. and Armbruster, T. (2000) Mg^{2+}, Mn^{2+}, Cd^{2+}, Sr^{2+} and Cu^{2+} exchange in heulandite single crystals: X-ray structure refinements. In C. Colella and F.A. Mumpton, Eds., Natural Zeolites for the Third Millennium, 119–138, De Frede Editore, Napoli, Italy.

Stolz, J., Yang, P., and Armbruster, T. (2000) Cd-exchanged heulandite: symmetry lowering and site preference. Microporous and Mesoporous Materials, 37, 233–242.

Tarasevich, Y.I. (1996) Use of natural adsorbents as decontamination agents for the elimination of the Chernobyl nuclear power plant consequences. Journal of Water Chemistry and Technology, 18, 6–9.

MANUSCRIPT RECEIVED JULY 11, 2002
MANUSCRIPT ACCEPTED NOVEMBER 1, 2002
MANUSCRIPT HANDLED BY ALESSANDRO GUALTIERI